Numerical Homogenization of Sand from Grain-level Simulations - Supplemental Material

YI-LU CHEN, ISTA, Austria
MICKAËL LY, ISTA, Austria
CHRIS WOJTAN, ISTA, Austria

CCS Concepts: • **Computing methodologies** → **Physical simulation**; **Animation**.

ACM Reference Format:
Yi-Lu Chen, Mickaël Ly, and Chris Wojtan. 2025. Numerical Homogenization of Sand from Grain-level Simulations - Supplemental Material. *ACM Trans. Graph.* 44, 6, Article 220 (December 2025), 22 pages. https://doi.org/10.1145/3763344

A Overview of homogenization theory

In this section, we will give a quick review of homogenization theory relevant to our work. We closely follows the work of de Souza Neto et al. [2015], and interested readers are also encouraged to read that paper.

A.1 Notations

Let Ω_0 and Ω closed subsets of $\mathbb{R}^3$ be our microscopic *representative volume element* (RVE) in material and world space respectively. For the remainder of the section, the bold capital and bold lowercase letters denote quantities in Ω_0 and in Ω respectively. We assume that they define triply-periodic boundary conditions *i.e.* $\exists \mathbf{A}, \mathbf{B}, \mathbf{C} \in \mathbb{R}^3 \backslash \{0\}$ such that the functions $f : \Omega_0 \mapsto \mathbb{R}^m$ we are interested in satisfy $\forall i, j, k \in \mathbb{Z}, \forall X \in \Omega_0 : f(\mathbf{X}) = f(\mathbf{X}+i\mathbf{A}+j\mathbf{B}+k\mathbf{C})$. This naturally defines "negative" and "positive" boundaries $\partial\Omega_0^-$ and $\partial\Omega_0^+$ of the RVE as $\partial\Omega_0^-, \partial\Omega_0^+ \subset \partial\Omega_0$ and $\partial\Omega_0^+ = \partial\Omega_0^- + i\mathbf{A} + j\mathbf{B} + k\mathbf{C}$ for $i, j, k \in \mathbb{N}$.

A.2 Displacement and deformation

The core idea behind homogenization is an assumption of multiple scales, a macroscale and a microscale. Displacements in the microscale are infinitesimally smaller than those at the macroscale, whereas the macroscale represents some "average" of properties at the microscale.

Let the two closed subsets of $\mathbb{R}^3$ Ω_0 and Ω be our microscopic *representative volume element* (RVE) in material space (μ_0) and world space (μ) respectively within a *macroscopic* continuum. At the macroscopic level, the RVE is then represented by its centroid $\mathbf{X}$ in material space. That is,

$$\mathbf{X} = \frac{1}{M_\Omega} \int_{\Omega_0} \rho_0(\mathbf{Y})\mathbf{Y} \, dV \tag{1}$$

Authors' Contact Information: Yi-Lu Chen, ISTA, Klosterneuburg, Austria, yi-lu.chen@ista.ac.at; Mickaël Ly, ISTA, Klosterneuburg, Austria, mickael.ly@ista.ac.at; Chris Wojtan, ISTA, Klosterneuburg, Austria, wojtan@ist.ac.at.

ACM 1557-7368/2025/12-ART220
https://doi.org/10.1145/3763344

where $\rho_0(\mathbf{Y})$ denotes the density at $\mathbf{Y}$ and $M_\Omega = \int_{\Omega_0} \rho_0(\mathbf{Y})\ dV$ is the total mass of the RVE. The two equations then results in

$$\int_{\Omega_0} \rho_0(\mathbf{Y})(\mathbf{Y} - \mathbf{X})\ dV = \mathbf{0} \tag{2}$$

Given a deformation, each position $\mathbf{Y}$ of the RVE then maps to a different position in world space $\mathbf{y} = \mathbf{Y} + \mathbf{u}(\mathbf{Y})$, with $\mathbf{u}(\mathbf{Y})$ denoting the *displacement* of $\mathbf{Y}$. A first-order Taylor expansion then gives

$$\mathbf{y} = \mathbf{x} + \mathbf{F_x}(\mathbf{Y} - \mathbf{X}) + \tilde{\mathbf{u}}(\mathbf{Y}) \tag{3}$$

where $\mathbf{F_x}$ denotes the *deformation gradient* at $\mathbf{X}$, and $\tilde{\mathbf{u}}(\mathbf{Y})$ denotes the *fluctuation field* in material space.

Taking the spatial derivative of Eq. 3 w.r.t. $\mathbf{Y}$ gives us the *micro-scale deformation gradient* at $\mathbf{Y}$

$$\mathbf{F}_{\mu_0}(\mathbf{Y}) := \frac{\partial \mathbf{y}}{\partial \mathbf{Y}} = \mathbf{F_x} + \nabla_{\mu_0}\tilde{\mathbf{u}}(\mathbf{Y}) \tag{4}$$

It is sometimes also convenient to consider the *Eulerian* view of displacement, especially when dealing with measurements solely defined in world space, such as Cauchy stresses. Let $\mathbf{u}^*$ and $\tilde{\mathbf{u}}^*$ be the displacement and fluctuation fields in *world coordinates*, respectively. Then similarly, a Taylor expansion yields

$$\mathbf{y} = \mathbf{x} + \mathbf{G_x}(\mathbf{y} - \mathbf{x}) + \tilde{\mathbf{u}}^*(\mathbf{y}) \Rightarrow \mathbf{G}_\mu(\mathbf{y}) := \nabla_\mu \mathbf{u}^*(\mathbf{y}) = \mathbf{G_x} + \nabla_\mu \tilde{\mathbf{u}}^*(\mathbf{y}) \tag{5}$$

where $\mathbf{G_x} = \frac{\partial \mathbf{u}}{\partial \mathbf{x}}$.

A.3 Kinematic admissibility

The core idea of multi-scale homogenization is that the displacement and deformation of $\mathbf{X}$ represents an average of all points $\mathbf{Y}$ in the RVE in some sense. Specifically, we postulate the following two properties: first that the displacement at the macroscopic level is a weighted average of the micro-displacements:

$$\mathbf{u}(\mathbf{X}) = \frac{1}{M_\Omega} \int_{\Omega_0} \rho_0(\mathbf{Y})\mathbf{u}(\mathbf{Y})\ dV \tag{6}$$

In some literature, the following alternative form is used instead by substituting Eq. 3 into Eq, 6 and using the relation in Eq. 2:

$$\begin{aligned}
\mathbf{u}(\mathbf{X}) &= \frac{1}{M_\Omega} \int_{\Omega_0} \rho_0(\mathbf{Y}) \left(\mathbf{u}(\mathbf{X}) + \mathbf{X} - \mathbf{Y} + \mathbf{F_x}(\mathbf{Y} - \mathbf{X}) + \tilde{\mathbf{u}}(\mathbf{Y}) \right)\ dV && (7)\\
&= \frac{1}{M_\Omega} \left(\int_{\Omega_0} \rho_0(\mathbf{Y})\mathbf{u}(\mathbf{X})\ dV + \int_{\Omega_0} (\mathbf{F_x} - \mathbf{I})(\mathbf{Y} - \mathbf{X})\ dV + \int_{\Omega_0} \tilde{\mathbf{u}}(\mathbf{Y})\ dV \right) && (8)\\
&= \mathbf{u}(\mathbf{X}) + \mathbf{0} + \frac{1}{M_\Omega} \int_{\Omega_0} \rho_0(\mathbf{Y})\tilde{\mathbf{u}}(\mathbf{Y})\ dV && (9)\\
\Rightarrow & \int_{\Omega_0} \rho_0(\mathbf{Y})\tilde{\mathbf{u}}(\mathbf{Y})\ dV = \mathbf{0} && (10)
\end{aligned}$$

Secondly, we assume the homogenized deformation gradient to be the average over the RVE. That is,

$$\mathbf{F_x} = \frac{1}{\|\Omega_0\|} \int_{\Omega_0} \mathbf{F}_{\mu_0}(\mathbf{y})\ dV \tag{11}$$

Substituting Eq. 4 into the above then gives

$$\mathbf{F_x} = \frac{1}{\|\Omega_0\|}\int_{\Omega_0} \mathbf{F_x} + \nabla_{\mu_0}\tilde{\mathbf{u}}(\mathrm{Y})\ dV = \mathbf{F_x} + \frac{1}{\|\Omega_0\|}\int_{\Omega_0} \nabla_{\mu_0}\tilde{\mathbf{u}}(\mathrm{Y})\ dV \tag{12}$$

$$\Rightarrow \int_{\Omega_0} \nabla_{\mu_0}\tilde{\mathbf{u}}(\mathrm{Y})\ dV = \mathbf{0} \tag{13}$$

Using Corollary B.2 from Sec. B, we have the following relation:

$$\int_{\Omega_0} \nabla_{\mu_0}\tilde{\mathbf{u}}(\mathrm{Y})\ dV = \int_{\partial\Omega_0} \tilde{\mathbf{u}}(\mathrm{Y}) \otimes \mathbf{n}\ dA \Rightarrow \int_{\partial\Omega_0} \tilde{\mathbf{u}}(\mathrm{Y}) \otimes \mathbf{n}\ dA = \mathbf{0}$$

The two assumptions above do not necessarily hold for any arbitrary representative volume. Therefore, one needs to be careful in designing the representative volume such that the two assumptions are guaranteed. In other words a fluctuation field is *kinematically admissible* if the two conditions hold:

$$\begin{cases} \int_{\Omega_0} \rho_0(\mathrm{Y})\tilde{\mathbf{u}}(\mathrm{Y})\ dV & = \mathbf{0} \\ \int_{\Omega_0} \nabla_{\mu_0}\tilde{\mathbf{u}}(\mathrm{Y})\ dV & = \mathbf{0} \qquad (\text{or } \int_{\partial\Omega_0} \tilde{\mathbf{u}}(\mathrm{Y}) \otimes \mathbf{n}\ dA = \mathbf{0}) \end{cases} \tag{14}$$

A.3.1 Rigid-body simulations in triply periodic boundaries are kinematically permissible. Assuming no external forces, since contact forces are equal and opposite for each pair of rigid bodies, the momentum of the RVE should be preserved, and $\mathbf{u}(\mathbf{X}) = 0$. We further have

$$\int_{\Omega_0} \rho_0(\mathrm{Y})\mathbf{v}(\mathrm{Y})\ dV = 0 \Rightarrow \int_{t_0}^{t}\int_{\Omega_0} \rho_0(\mathrm{Y})\mathbf{v}(\mathrm{Y})\ dV\ dt = \int_{\Omega_0} \rho_0(\mathrm{Y}) \int_{t_0}^{t} \mathbf{v}(\mathrm{Y})\ dt\ dV = \int_{\Omega_0} \rho_0(\mathrm{Y})\mathbf{u}(\mathrm{Y})\ dV = \mathbf{0}$$

where $\mathbf{v}(\mathrm{Y})$ denotes the velocity at point $\mathbf{Y}$, the first condition is thus fulfilled. Additionally, any fluctuation on the boundary has an identical fluctuation on a corresponding periodic boundary by definition, while both points have opposite-facing normals. We then have

$$\begin{aligned} \int_{\partial\Omega_0} \tilde{\mathbf{u}}(\mathrm{Y}) \otimes \mathbf{n}\ dA &= \int_{\partial\Omega_0^+} \tilde{\mathbf{u}}(\mathrm{Y}) \otimes \mathbf{n}\ dA + \int_{\partial\Omega_0^-} \tilde{\mathbf{u}}(\mathrm{Y}) \otimes \mathbf{n}\ dA \\ &= \int_{\partial\Omega_0^+} \tilde{\mathbf{u}}(\mathrm{Y}) \otimes \mathbf{n}\ dA + \int_{\partial\Omega_0^+} \tilde{\mathbf{u}}(\mathrm{Y}) \otimes -\mathbf{n}\ dA = \mathbf{0} \end{aligned}$$

fulfilling the second condition. This shows that rigid-body simulations on periodic boundary conditions are kinematically admissible.

A.4 Homogenized stress and the principle of multi-scale virtual power

The *principle of multi-scale virtual power*, also known as the *Hill–Mandel Principle* [Hill 1963, 1972; Mandel 1972], states that a usable homogenization of stress induces the same amount of work at both the macroscopic level and the microscopic one. That is, for any infinitesimal deformation field $\delta\mathbf{F}$, we have

$$\|\Omega_0\|\ (\bar{\mathbf{P}} : \delta\mathbf{F}) = \int_{\Omega_0} \mathbf{P} : \delta\mathbf{F}_\mu\ dV \tag{15}$$

where $\bar{\mathbf{P}}$ and $\mathbf{P}$ are the macroscopic and microscopic first Piola–Kirchhoff stress tensors, respectively.

For any kinematically admissible fluctuation field, this implies that

$$\left\|\Omega_\mu\right\|\ (\bar{\mathbf{P}} : \delta\mathbf{F}) = \int_{\Omega_\mu} \mathbf{P} : (\delta\mathbf{F} + \nabla_{\mu_0}\delta\tilde{\mathbf{u}})\ dV \tag{16}$$

Since $\delta\tilde{\mathbf{u}}_\mu = \mathbf{0}$ is kinematically permissible, applying it to the above equation gives

$$\left\|\Omega_\mu\right\| (\bar{\mathbf{P}} : \delta\mathbf{F}) = \int_{\Omega_\mu} \mathbf{P}\; dV : \delta\mathbf{F} \tag{17}$$

for all $\delta\mathbf{F}$, so

$$\bar{\mathbf{P}} = \frac{1}{\left\|\Omega_\mu\right\|} \int_{\Omega_\mu} \mathbf{P}\; dV \tag{18}$$

Similarly, setting $\delta\mathbf{F} = \mathbf{0}$ results in

$$\int_{\Omega_\mu} \mathbf{P}_\mu : \nabla_\mu \tilde{\mathbf{u}}_\mu \; dV = 0 \tag{19}$$

for all kinematically permissible fluctuations.

In world space, a similar argument from virtual work can be constructed with an infinitesimal displacement gradient field $\delta\mathbf{G}$:

$$\|\Omega\| \, (\bar{\boldsymbol{\sigma}} : \delta\mathbf{G}) = \int_\Omega \boldsymbol{\sigma} : \delta\mathbf{G}_\mu \; dv \tag{20}$$

$$= \int_\Omega \boldsymbol{\sigma} : (\delta\mathbf{G} + \nabla_\mu \tilde{\mathbf{u}}^*(\mathbf{y})) \; dv \tag{21}$$

$$\bar{\boldsymbol{\sigma}} = \frac{1}{\|\Omega\|} \int_\Omega \boldsymbol{\sigma}\; dv \tag{22}$$

B Divergence theorem corollaries

The divergence theorem, which holds for higher-order tensors, is given as

Theorem B.1. *(Divergence theorem) For any smooth vector field* $\mathbf{v}$*,*

$$\int_V \operatorname{div} \mathbf{v}\; dV = \int_{\partial V} \mathbf{v}\mathbf{n}\; dA$$

This generalizes to any higher order tensor field in Cartesian coordinates as the following for any tensor and normal components

$$\int_V \frac{\partial \sigma_{i_1, i_2, \ldots i_d}}{\partial x_{i_k}} \; dV = \int_{\partial V} \sigma_{i_1, i_2, \ldots i_d} n_{i_k} \; dA$$

The following corollaries are used in this text, with summation implied over indices in the proofs.

Corollary B.2. *For any vector field* $\mathbf{v}$*,*

$$\int_{\partial V} \mathbf{v} \otimes \mathbf{n}\; dA = \int_V \nabla \mathbf{v}\; dV$$

Proof. We have $\mathbf{v} \otimes \mathbf{n} = v_i n_j \mathbf{e_{ij}} = w_{ijk} n_j \mathbf{e_{ij}}$, where $w_{ijk} = \delta_{jk} v_i$. Therefore,

$$\int_{\partial V} \mathbf{v} \otimes \mathbf{n}\; dA = \int_{\partial V} w_{ijk} n_j \mathbf{e_{ij}}\; dA = \int_V \frac{\partial w_{ijk}}{\partial \mathbf{x}_j} \mathbf{e_{ij}}\; dV = \int_V \delta_{jk} \frac{\partial v_i}{\partial \mathbf{x}_j} \mathbf{e_{ij}}\; dV = \int_V \nabla \mathbf{v}\; dV$$

□

Corollary B.3. *For any smooth tensor field* $\boldsymbol{\sigma}$*,*

$$\int_V \boldsymbol{\sigma}\; dV = \int_{\partial V} (\boldsymbol{\sigma}\mathbf{n}) \otimes \mathbf{x}\; dA - \int_V (\nabla \cdot \boldsymbol{\sigma}) \otimes \mathbf{x}\; dV$$

Proof.

$$
\begin{aligned}
(\boldsymbol{\sigma}\mathbf{n}) \otimes \mathbf{x} &= \sigma_{ik} n_k x_j \mathbf{e_{ij}} \\
\Rightarrow \int_{\partial V} (\boldsymbol{\sigma}\mathbf{n}) \otimes \mathbf{x} &= \int_{\partial V} \sigma_{ik} x_j n_k \mathbf{e_{ij}} \; dA \\
&= \int_V \frac{\partial \sigma_{ik} x_j}{\partial x_k} \mathbf{e_{ij}} \; dV \\
&= \int_V \frac{\partial \sigma_{ik}}{\partial x_k} x_j \mathbf{e_{ij}} + \sigma_{ik} \frac{\partial x_j}{\partial x_k} \mathbf{e_{ij}} \; dV \\
&= \int_V \frac{\partial \sigma_{ik}}{\partial x_k} x_j \mathbf{e_{ij}} + \sigma_{ik} \delta_{jk} \mathbf{e_{ij}} \; dV \\
&= \int_V \frac{\partial \sigma_{ik}}{\partial x_k} x_j \mathbf{e_{ij}} + \sigma_{ij} \mathbf{e_{ij}} \; dV \\
&= \int_V (\nabla \cdot \boldsymbol{\sigma}) \otimes \mathbf{x} + \boldsymbol{\sigma} \; dV
\end{aligned}
$$

And so $\int_V \boldsymbol{\sigma} \; dV = \int_{\partial V} (\boldsymbol{\sigma}\mathbf{n}) \otimes \mathbf{x} \; dA - \int_V (\nabla \cdot \boldsymbol{\sigma}) \otimes \mathbf{x} \; dV$ □

C Closed-form solution of second mass moment for closed triangle meshes

Let V be a volume enclosed by a manifold triangle mesh M with a center of mass $\mathbf{x}^*$. We want to evaluate the second mass moment of M. That is, evaluate

$$\int_V \rho \left\|\mathbf{x}-\mathbf{x}^*\right\|^2 \ dV$$

assuming the density ρ is uniform in V.

Let T_i be the i-th triangle in M, and $V_i = \operatorname{conv}(T_i, \mathbf{x}^*)$ be the convex hull of the vertices of T_i and $\mathbf{x}^*$, i.e. the tetrahedron formed by the four vertices. We can observe that the integral can be decomposed into the sum

$$\int_V \rho \left\|\mathbf{x}-\mathbf{x}^*\right\|^2 \ dV = \rho \sum_i \operatorname{sign}\left((\mathbf{x}_\mathbf{i}^* - \mathbf{x}^*)\cdot \mathbf{n_i}\right) \int_{V_i} \left\|\mathbf{x}-\mathbf{x}^*\right\|^2 \ dV \tag{23}$$

where $\mathbf{x}_\mathbf{i}^*$ denotes the center of mass of the triangle T_i, and $\mathbf{n_i}$ its outward-pointing normal.

To evaluate the intergral on the right hand side of Eq. 23, assume that the integral $\int_{T_i} \left\|\mathbf{x}-\mathbf{x}^*\right\|^2 \ dA$ is known, and that $(\mathbf{x}_\mathbf{i}^* - \mathbf{x}^*)\cdot \mathbf{n_i} \geq 0$. We now consider the integral of a new triangle $T_i(a)$, where any point $\mathbf{x} \in T_i$ is scaled to a new point on $T_i(a)$ as $\mathbf{x}' = \mathbf{x}^* + a(\mathbf{x}-\mathbf{x}^*)$ for some scale $a \geq 0$. Then

$$\int_{T_i(a)} \left\|\mathbf{x}-\mathbf{x}^*\right\|^2 \ dA = \int_{T_i} \left\|\mathbf{x}^* + a(\mathbf{x}-\mathbf{x}^*) - \mathbf{x}^*\right\|^2 \ a^2 dA = a^4 \int_{T_i} \left\|\mathbf{x}-\mathbf{x}^*\right\|^2 \ dA$$

The integral over the tetrahedron can then be thought of as an integral over these scaled triangles:

$$\begin{aligned}
\int_{V_i} \left\|\mathbf{x}-\mathbf{x}^*\right\|^2 \ dV &= \int_0^{(\mathbf{x}_\mathbf{i}^*-\mathbf{x}^*)\cdot\mathbf{n_i}} \int_{T_i(y/(\mathbf{x}_\mathbf{i}^*-\mathbf{x}^*)\cdot\mathbf{n_i})} \left\|\mathbf{x}-\mathbf{x}^*\right\|^2 \ dA\ dy \\
&= \int_0^1 \int_{T_i(z)} \left\|\mathbf{x}-\mathbf{x}^*\right\|^2 \ dA\ (\mathbf{x}_\mathbf{i}^* - \mathbf{x}^*)\cdot \mathbf{n_i} dz \\
&= \int_0^1 z^4 \int_{T_i} \left\|\mathbf{x}-\mathbf{x}^*\right\|^2 \ dA\ (\mathbf{x}_\mathbf{i}^* - \mathbf{x}^*)\cdot \mathbf{n_i} dz \\
&= \frac{(\mathbf{x}_\mathbf{i}^* - \mathbf{x}^*)\cdot \mathbf{n_i}}{5} \int_{T_i} \left\|\mathbf{x}-\mathbf{x}^*\right\|^2 \ dA
\end{aligned}$$

We denote $H_i := (\mathbf{x}_\mathbf{i}^* - \mathbf{x}^*)\cdot \mathbf{n_i}$. Notice that since H_i accounts for the sign() function in Eq. 23, it can be simplified to

$$\int_V \rho \left\|\mathbf{x}-\mathbf{x}^*\right\|^2 \ dV = \rho \sum_i \frac{H_i}{5} \int_{T_i} \left\|\mathbf{x}-\mathbf{x}^*\right\|^2 \ dA \tag{24}$$

We then simplify the integral on the right hand side with

$$\begin{aligned}
\int_{T_i} \left\|\mathbf{x}-\mathbf{x}^*\right\|^2 \ dA &= \int_{T_i} \left\|(\mathbf{x}-\mathbf{x}_\mathbf{i}^*) + (\mathbf{x}_\mathbf{i}^* - \mathbf{x}^*)\right\|^2 \ dA \\
&= \int_{T_i} \left\|\mathbf{x}-\mathbf{x}_\mathbf{i}^*\right\|^2 + 2(\mathbf{x}-\mathbf{x}_\mathbf{i}^*)\cdot(\mathbf{x}_\mathbf{i}^* - \mathbf{x}^*) + \left\|\mathbf{x}_\mathbf{i}^* - \mathbf{x}^*\right\|^2 \ dA \\
&= \int_{T_i} \left\|\mathbf{x}-\mathbf{x}_\mathbf{i}^*\right\|^2 \ dA + \int_{T_i} \left\|\mathbf{x}_\mathbf{i}^* - \mathbf{x}^*\right\|^2 \ dA + 2(\mathbf{x}_\mathbf{i}^* - \mathbf{x}^*)\cdot \int_{T_i} (\mathbf{x}-\mathbf{x}_\mathbf{i}^*)\ dA \\
&= \int_{T_i} \left\|\mathbf{x}-\mathbf{x}_\mathbf{i}^*\right\|^2 \ dA + \|T_i\| \left\|\mathbf{x}_\mathbf{i}^* - \mathbf{x}^*\right\|^2
\end{aligned} \tag{25}$$

with the third term vanishing since $\int_{T_i} \mathbf{x}\ dA = \int_{T_i} \mathbf{x}_\mathbf{i}^*\ dA$ by definition.

We now use a similar trick to evaluate $\int_{T_i} \left\|\mathbf{x} - \mathbf{x_i^*}\right\|^2 \, dA$: we split up T_i into three triangles $T_i^1 = \mathrm{conv}(\mathbf{x_i^2}, \mathbf{x_i^3}, \mathbf{x_i^*})$, $T_i^2 = \mathrm{conv}(\mathbf{x_i^1}, \mathbf{x_i^3}, \mathbf{x_i^*})$, $T_i^3 = \mathrm{conv}(\mathbf{x_i^1}, \mathbf{x_i^2}, \mathbf{x_i^*})$, and denote the bases of each triangle with $L_i^1 = \mathrm{conv}(\mathbf{x_i^2}, \mathbf{x_i^3})$, $L_i^2 = \mathrm{conv}(\mathbf{x_i^3}, \mathbf{x_i^1})$, $L_i^3 = \mathrm{conv}(\mathbf{x_i^1}, \mathbf{x_i^2})$, as well as the heights $H_i^j = 2\frac{\left\|T_i^j\right\|}{\left\|L_i^j\right\|} = \frac{2}{3}\frac{\|T_i\|}{\left\|L_i^j\right\|}$. We now have

$$
\begin{aligned}
\int_{T_i} \left\|\mathbf{x} - \mathbf{x_i^*}\right\|^2 \, dA &= \sum_{j=1}^{3} \int_{T_i^j} \left\|\mathbf{x} - \mathbf{x_i^*}\right\|^2 \, dA \\
&= \sum_{j=1}^{3} \int_0^1 z^3 \int_{L_i^j} \left\|\mathbf{x} - \mathbf{x_i^*}\right\|^2 \, dL \; H_i^j dz \\
&= \sum_{j=1}^{3} \frac{H_i^j}{4} \int_{L_i^j} \left\|\mathbf{x} - \mathbf{x_i^*}\right\|^2 \, dL
\end{aligned} \tag{26}
$$

By letting $\mathbf{m_i^j}$ denote the midpoint of L_i^j, we have

$$
\begin{aligned}
\int_{L_i^j} \left\|\mathbf{x} - \mathbf{x_i^*}\right\|^2 \, dL &= \int_{L_i^j} \left\|(\mathbf{x} - \mathbf{m_i^j}) + (\mathbf{m_i^j} - \mathbf{x_i^*})\right\|^2 \, dL \\
&= \int_{L_i^j} \left\|\mathbf{x} - \mathbf{m_i^j}\right\|^2 + \left\|\mathbf{m_i^j} - \mathbf{x_i^*}\right\|^2 + 2(\mathbf{x} - \mathbf{m_i^j}) \cdot (\mathbf{m_i^j} - \mathbf{x_i^*}) \, dL \\
&= \int_{L_i^j} \left\|\mathbf{x} - \mathbf{m_i^j}\right\|^2 \, dL + \left\|L_i^j\right\| \left\|\mathbf{m_i^j} - \mathbf{x_i^*}\right\|^2
\end{aligned} \tag{27}
$$

Again, the last term vanishes since $\int_{L_i^j} \mathbf{x} \, dL = \int_{L_i^j} \mathbf{m_i^j} \, dL$.

The remaining integral now has a closed-form solution

$$
\int_{L_i^j} \left\|\mathbf{x} - \mathbf{m_i^j}\right\|^2 \, dL = 2 \int_0^{\left\|L_i^j\right\|/2} y^2 \, dy = \left. \frac{2}{3} y^3 \right|_0^{\left\|L_i^j\right\|/2} = \frac{\left\|L_i^j\right\|^3}{12} \tag{28}
$$

which we can substitute back into Eq. 27:

$$
\begin{aligned}
\int_{L_i^j} \left\|\mathbf{x} - \mathbf{x_i^*}\right\|^2 \, dL &= \int_{L_i^j} \left\|\mathbf{x} - \mathbf{m_i^j}\right\|^2 \, dL + \left\|L_i^j\right\| \left\|\mathbf{m_i^j} - \mathbf{x_i^*}\right\|^2 \\
&= \left\|L_i^j\right\| \left(\frac{\left\|L_i^j\right\|^2}{12} + \left\|\mathbf{m_i^j} - \mathbf{x_i^*}\right\|^2 \right)
\end{aligned} \tag{29}
$$

Substituting Eq. 29 into Eq. 26 gives

$$
\begin{aligned}
\int_{T_i} \left\|\mathbf{x}-\mathbf{x_i^*}\right\|^2 \ dA &= \sum_{j=1}^{3} \frac{H_i^j}{4} \int_{L_i^j} \left\|\mathbf{x}-\mathbf{x_i^*}\right\|^2 \ dL \\
&= \sum_{j=1}^{3} \frac{H_i^j}{4} \left\|L_i^j\right\| \left(\frac{\left\|L_i^j\right\|^2}{12} + \left\|\mathbf{m_i^j}-\mathbf{x_i^*}\right\|^2 \right) \\
&= \sum_{j=1}^{3} \frac{1}{4} \cdot \frac{2}{3} \frac{\|T_i\|}{\left\|L_i^j\right\|} \left\|L_i^j\right\| \left(\frac{\left\|L_i^j\right\|^2}{12} + \left\|\mathbf{m_i^j}-\mathbf{x_i^*}\right\|^2 \right) \\
&= \frac{\|T_i\|}{6} \sum_{j=1}^{3} \left(\frac{\left\|L_i^j\right\|^2}{12} + \left\|\mathbf{m_i^j}-\mathbf{x_i^*}\right\|^2 \right)
\end{aligned} \tag{30}
$$

We now define $\mathbf{y_i^j} = \mathbf{x_i^j} - \mathbf{x_i^*}$. Now Eq. 30 can be simplified with

$$
\begin{aligned}
\sum_{j=1}^{3} \left(\frac{\left\|L_i^j\right\|^2}{12} + \left\|\mathbf{m_i^j}-\mathbf{x_i^*}\right\|^2 \right) &= \sum_{j=1}^{2} \sum_{k=j+1}^{3} \frac{1}{12} \left\|\mathbf{y_i^j}-\mathbf{y_i^k}\right\|^2 + \sum_{j=1}^{2} \sum_{k=j+1}^{3} \left\| \frac{\mathbf{y_i^j}+\mathbf{y_i^k}}{2} \right\|^2 \\
&= 2 \cdot \left(\frac{1}{12} + \frac{1}{4} \right) \sum_{j=1}^{3} \left\|\mathbf{y_i^j}\right\|^2 + \left(\frac{-1}{6} + \frac{1}{2} \right) \sum_{j=1}^{2} \sum_{k=j+1}^{3} \mathbf{y_i^j} \cdot \mathbf{y_i^k} \\
&= \frac{2}{3} \sum_{j=1}^{3} \left\|\mathbf{y_i^j}\right\|^2 + \frac{1}{3} \sum_{j=1}^{2} \sum_{k=j+1}^{3} \mathbf{y_i^j} \cdot \mathbf{y_i^k} \\
&= \frac{2}{3} \sum_{j=1}^{3} \left\|\mathbf{y_i^j}\right\|^2 + \frac{4}{3} \sum_{j=1}^{2} \sum_{k=j+1}^{3} \mathbf{y_i^j} \cdot \mathbf{y_i^k} - \sum_{j=1}^{2} \sum_{k=j+1}^{3} \mathbf{y_i^j} \cdot \mathbf{y_i^k} \\
&= \frac{2}{3} \left\|\mathbf{y_i^1}+\mathbf{y_i^2}+\mathbf{y_i^3}\right\|^2 - \sum_{j=1}^{2} \sum_{k=j+1}^{3} \mathbf{y_i^j} \cdot \mathbf{y_i^k} \\
&= \frac{2}{3} \left\|\mathbf{x_i^1}+\mathbf{x_i^2}+\mathbf{x_i^3}-3\mathbf{x_i^*}\right\|^2 - \sum_{j=1}^{2} \sum_{k=j+1}^{3} \mathbf{y_i^j} \cdot \mathbf{y_i^k} \\
&= -\sum_{j=1}^{2} \sum_{k=j+1}^{3} \mathbf{y_i^j} \cdot \mathbf{y_i^k}
\end{aligned}
$$

$$
\Rightarrow \int_{T_i} \left\|\mathbf{x}-\mathbf{x_i^*}\right\|^2 \ dA = \frac{-\|T_i\|}{6} \sum_{j=1}^{2} \sum_{k=j+1}^{3} \mathbf{y_i^j} \cdot \mathbf{y_i^k} \tag{31}
$$

which when substituted into Eq. 25 gives

$$\begin{aligned}\int_{T_i} \|\mathbf{x}-\mathbf{x}^*\|^2 \; dA &= \int_{T_i} \left\|\mathbf{x}-\mathbf{x}_\mathbf{i}^*\right\|^2 \; dA + \|T_i\| \left\|\mathbf{x}_\mathbf{i}^*-\mathbf{x}^*\right\|^2 \\ &= \|T_i\| \left\|\mathbf{x}_\mathbf{i}^*-\mathbf{x}^*\right\|^2 - \frac{\|T_i\|}{6} \sum_{j=1}^{2} \sum_{k=j+1}^{3} \mathbf{y}_\mathbf{i}^\mathbf{j} \cdot \mathbf{y}_\mathbf{i}^\mathbf{k}\end{aligned} \tag{32}$$

and so, by noting that the *signed* volume of tetrahedron i is $\|V_i\| = \frac{1}{3} H_i \|T_i\|$ we arrive at

$$\begin{aligned}\int_V \rho \|\mathbf{x}-\mathbf{x}^*\|^2 \; dV &= \rho \sum_i \frac{H_i}{5} \int_{T_i} \|\mathbf{x}-\mathbf{x}^*\|^2 \; dA \\ &= \rho \sum_i \frac{H_i \|T_i\|}{5} \left(\left\|\mathbf{x}_\mathbf{i}^*-\mathbf{x}^*\right\|^2 - \frac{1}{6} \sum_{j=1}^{2} \sum_{k=j+1}^{3} \mathbf{y}_\mathbf{i}^\mathbf{j} \cdot \mathbf{y}_\mathbf{i}^\mathbf{k} \right) \\ &= \rho \sum_i \frac{3\|V_i\|}{5} \left(\left\|\mathbf{x}_\mathbf{i}^*-\mathbf{x}^*\right\|^2 - \frac{1}{6} \sum_{j=1}^{2} \sum_{k=j+1}^{3} \mathbf{y}_\mathbf{i}^\mathbf{j} \cdot \mathbf{y}_\mathbf{i}^\mathbf{k} \right) \\ &= \rho \sum_i \frac{\|V_i\|}{10} \left(6\left\|\mathbf{x}_\mathbf{i}^*-\mathbf{x}^*\right\|^2 - \sum_{j=1}^{2} \sum_{k=j+1}^{3} \mathbf{y}_\mathbf{i}^\mathbf{j} \cdot \mathbf{y}_\mathbf{i}^\mathbf{k} \right)\end{aligned} \tag{33}$$

We can further simplify the expression and remove $\mathbf{y}_\mathbf{i}^\cdot$ by noting that for each tetrahedron, its center of mass lies on $\frac{1}{4}\mathbf{x}^* + \frac{3}{4}\mathbf{x}_\mathbf{i}^*$, and we have the relation

$$\sum_i \|V_i\| \left(\frac{1}{4}\mathbf{x}^* + \frac{3}{4}\mathbf{x}_\mathbf{i}^* \right) = \|V\| \, \mathbf{x}^* \Rightarrow \sum_i \|V_i\| \, \mathbf{x}_\mathbf{i}^* = \|V\| \, \mathbf{x}^*$$

hence

$$
\begin{aligned}
\int_V \rho \left\|\mathbf{x}-\mathbf{x}^*\right\|^2 \, dV &= \rho \sum_i \frac{\|V_i\|}{10}\left(6\left\|\mathbf{x_i^*}-\mathbf{x}^*\right\|^2 - \sum_{j=1}^{2}\sum_{k=j+1}^{3} \mathbf{y_i^j}\cdot\mathbf{y_i^k}\right)\\
&= \rho \sum_i \frac{\|V_i\|}{10}\left(6\left\|\mathbf{x_i^*}-\mathbf{x}^*\right\|^2 - \sum_{j=1}^{2}\sum_{k=j+1}^{3} (\mathbf{x_i^j}-\mathbf{x_i^*})\cdot(\mathbf{x_i^k}-\mathbf{x_i^*})\right)\\
&= \rho \sum_i \frac{\|V_i\|}{10}\left(6\left(\left\|\mathbf{x_i^*}\right\|^2+\left\|\mathbf{x}^*\right\|^2-2\mathbf{x_i^*}\cdot\mathbf{x}^*\right) - \sum_{j=1}^{2}\sum_{k=j+1}^{3} (\mathbf{x_i^j}-\mathbf{x_i^*})\cdot(\mathbf{x_i^k}-\mathbf{x_i^*})\right)\\
&= \rho \sum_i \frac{\|V_i\|}{10}\left(6\left(\left\|\mathbf{x_i^*}\right\|^2+\left\|\mathbf{x}^*\right\|^2-2\mathbf{x_i^*}\cdot\mathbf{x}^*\right) - \sum_{j=1}^{2}\sum_{k=j+1}^{3} \mathbf{x_i^j}\cdot\mathbf{x_i^k} - 3\left\|\mathbf{x_i^*}\right\|^2 + 2\mathbf{x_i^*}\cdot\sum_{j=1}^{3}\mathbf{x_i^j}\right)\\
&= \rho \sum_i \frac{\|V_i\|}{10}\left(6\left(\left\|\mathbf{x_i^*}\right\|^2+\left\|\mathbf{x}^*\right\|^2-2\mathbf{x_i^*}\cdot\mathbf{x}^*\right) - \sum_{j=1}^{2}\sum_{k=j+1}^{3} \mathbf{x_i^j}\cdot\mathbf{x_i^k} - 3\left\|\mathbf{x_i^*}\right\|^2 + 6\left\|\mathbf{x_i^*}\right\|^2\right)\\
&= \rho \sum_i \frac{\|V_i\|}{10}\left(9\left\|\mathbf{x_i^*}\right\|^2+6\left\|\mathbf{x}^*\right\|^2-12\mathbf{x_i^*}\cdot\mathbf{x}^* - \sum_{j=1}^{2}\sum_{k=j+1}^{3} \mathbf{x_i^j}\cdot\mathbf{x_i^k}\right)\\
&= \frac{9\rho}{10}\sum_i \|V_i\|\left\|\mathbf{x_i^*}\right\|^2 + \frac{6\rho}{10}\sum_i \|V_i\|\left\|\mathbf{x}^*\right\|^2 - \frac{12\rho}{10}\mathbf{x}^*\cdot\sum_i \|V_i\|\,\mathbf{x_i^*} - \frac{\rho}{10}\sum_i \|V_i\|\sum_{j=1}^{2}\sum_{k=j+1}^{3} \mathbf{x_i^j}\cdot\mathbf{x_i^k}\\
&= \frac{9\rho}{10}\sum_i \|V_i\|\left\|\mathbf{x_i^*}\right\|^2 - \frac{6\rho}{10}\|V\|\left\|\mathbf{x}^*\right\|^2 - \frac{\rho}{10}\sum_i \|V_i\|\sum_{j=1}^{2}\sum_{k=j+1}^{3} \mathbf{x_i^j}\cdot\mathbf{x_i^k}\\
&= \frac{\rho}{10}\left(\sum_i \|V_i\|\left(9\left\|\mathbf{x_i^*}\right\|^2 - \sum_{j=1}^{2}\sum_{k=j+1}^{3} \mathbf{x_i^j}\cdot\mathbf{x_i^k}\right) - 6\|V\|\left\|\mathbf{x}^*\right\|^2\right)\\
&= \frac{\rho}{10}\left(\sum_i \|V_i\|\left(\left\|\mathbf{x_i^1}+\mathbf{x_i^2}+\mathbf{x_i^3}\right\|^2 - \sum_{j=1}^{2}\sum_{k=j+1}^{3} \mathbf{x_i^j}\cdot\mathbf{x_i^k}\right) - 6\|V\|\left\|\mathbf{x}^*\right\|^2\right)\\
&= \frac{\rho}{10}\left(\sum_i \|V_i\|\left(\sum_{j=1}^{3}\left\|\mathbf{x_i^j}\right\|^2 + 2\sum_{j=1}^{2}\sum_{k=j+1}^{3} \mathbf{x_i^j}\cdot\mathbf{x_i^k} - \sum_{j=1}^{2}\sum_{k=j+1}^{3} \mathbf{x_i^j}\cdot\mathbf{x_i^k}\right) - 6\|V\|\left\|\mathbf{x}^*\right\|^2\right)\\
&= \frac{\rho}{10}\left(\sum_i \|V_i\|\left(\sum_{j=1}^{3}\left\|\mathbf{x_i^j}\right\|^2 + \sum_{j=1}^{2}\sum_{k=j+1}^{3} \mathbf{x_i^j}\cdot\mathbf{x_i^k}\right) - 6\|V\|\left\|\mathbf{x}^*\right\|^2\right)\\
&= \frac{\rho}{10}\left(\sum_i \sum_{j=1}^{3}\sum_{k=j}^{3} \|V_i\|\,\mathbf{x_i^j}\cdot\mathbf{x_i^k} - 6\|V\|\left\|\mathbf{x}^*\right\|^2\right)
\end{aligned} \tag{34}
$$

Finally, in the special case where $\mathbf{x}^* = \mathbf{0}$, $\|V_i\| = \frac{1}{6}\mathbf{x_i^1}\cdot(\mathbf{x_i^2}\times\mathbf{x_i^3})$, and

$$\int_V \rho \|\mathbf{x}\|^2 \; dV = \frac{\rho}{10} \sum_i \sum_{j=1}^{3} \sum_{k=j}^{3} \|V_i\| \, \mathbf{x_i^j} \cdot \mathbf{x_i^k}$$
$$= \frac{\rho}{60} \sum_i \mathbf{x_i^1} \cdot (\mathbf{x_i^2} \times \mathbf{x_i^3}) \sum_{j=1}^{3} \sum_{k=j}^{3} \mathbf{x_i^j} \cdot \mathbf{x_i^k} \tag{35}$$

D Dissipation under plastic deformation

Under multiplicative plasticity, a deformation tensor is decomposed into $\mathbf{F} = \mathbf{F}_E \mathbf{F}_P$. Assuming a hyperelastic solid, the first Piola–Kirchhoff stress tensor $\mathbf{P}$ can be calculated via chain rule:

$$\mathbf{P} = \frac{\partial \psi(\mathbf{F}_E)}{\partial \mathbf{F}} = \frac{\partial \psi(\mathbf{F}_E)}{\partial \mathbf{F}_E} \frac{\partial \mathbf{F}_E}{\partial \mathbf{F}} = \frac{\partial \psi(\mathbf{F}_E)}{\partial \mathbf{F}_E} \frac{\partial (\mathbf{F}\mathbf{F}_P^{-1})}{\partial \mathbf{F}} = \frac{\partial \psi(\mathbf{F}_E)}{\partial \mathbf{F}_E} \mathbf{F}_P^{-\top} \tag{36}$$

In terms of the Kirchhoff stress tensor $\boldsymbol{\tau}$, this can be rewritten as:

$$\boldsymbol{\tau} = \mathbf{P}\mathbf{F}^\top = \frac{\partial \psi(\mathbf{F}_E)}{\partial \mathbf{F}_E} \mathbf{F}_P^{-\top} \mathbf{F}^\top = \frac{\partial \psi(\mathbf{F}_E)}{\partial \mathbf{F}_E} \mathbf{F}_P^{-\top} \mathbf{F}_P^\top \mathbf{F}_E^\top = \frac{\partial \psi(\mathbf{F}_E)}{\partial \mathbf{F}_E} \mathbf{F}_E^\top \tag{37}$$

The following time derivatives of deformation gradients can then be derived with the product rule:

$$\begin{aligned}
\dot{\mathbf{F}} &= \dot{\mathbf{F}}_E \mathbf{F}_P + \mathbf{F}_E \dot{\mathbf{F}}_P \\
\dot{\mathbf{F}}_E &= \dot{\mathbf{F}} \mathbf{F}_P^{-1} - \mathbf{F}_E \dot{\mathbf{F}}_P \mathbf{F}_P^{-1} \\
\dot{\mathbf{F}}_P &= \mathbf{F}_E^{-1} \dot{\mathbf{F}} - \mathbf{F}_E^{-1} \dot{\mathbf{F}}_E \mathbf{F}_P
\end{aligned}$$

We further decompose the velocity gradient in world space into two parts $\nabla \mathbf{v} = \nabla \mathbf{v}_E + \nabla \mathbf{v}_P$, such that $\dot{\mathbf{F}}_E = \nabla \mathbf{v}_E \mathbf{F}_E$. Assuming $\mathbf{F}_E$ is not degenerate, such a tensor can always be found with $\mathbf{l}_E = \dot{\mathbf{F}}_E \mathbf{F}_E^{-1}$.

Let $\dot{E}_E$ be the time derivative of the total elastic potential. We have:

$$\dot{E}_E = \frac{\partial}{\partial t} \int_{\Omega_0} \psi(\mathbf{F}_E) \; dV_0 = \int_{\Omega_0} \frac{\partial \psi(\mathbf{F}_E)}{\partial \mathbf{F}_E} : \dot{\mathbf{F}}_E \; dV_0$$

where Ω_0 is the elastic body in *material* space. Using Eq. 36, we further have:

$$\begin{aligned}
\frac{\partial \psi}{\partial \mathbf{F}_E} : \dot{\mathbf{F}}_E &= \frac{\partial \psi}{\partial \mathbf{F}_E} \left(\mathbf{F}_P^{-\top} \mathbf{F}_P^\top \right) : \dot{\mathbf{F}}_E \left(\mathbf{F}_E^{-1} \mathbf{F}_E \right) \\
&= \left(\frac{\partial \psi}{\partial \mathbf{F}_E} \mathbf{F}_P^{-\top} \right) \left(\mathbf{F}_P^\top \mathbf{F}_E^\top \right) : \dot{\mathbf{F}}_E \mathbf{F}_E^{-1} \\
&= \mathbf{P}\mathbf{F}^\top : \dot{\mathbf{F}}_E \mathbf{F}_E^{-1} \\
&= \boldsymbol{\tau} : \nabla \mathbf{v}_E
\end{aligned}$$

Finally, let $\dot{W} = \int_\Omega \rho \mathbf{a} \cdot \mathbf{v} \; dV$ be the time derivative of work exerted on the elastic body, Ω be the elastic body in *world* space, and ρ, $\mathbf{a}$, $\mathbf{v}$ be the density, acceleration, and velocity of a point in the elastic body, respectively. $\dot{W}$

can then be rewritten with respect to the Cauchy stress $\boldsymbol{\sigma}$ via integration by parts:

$$
\begin{aligned}
\dot{W} &= \int_\Omega \rho \mathbf{a} \cdot \mathbf{v} \; dV = \int_\Omega (\nabla \cdot \boldsymbol{\sigma}) \cdot \mathbf{v} \; dV = \int_\Omega \nabla \cdot (\boldsymbol{\sigma}\mathbf{v}) - \boldsymbol{\sigma} : \nabla \mathbf{v} \; dV \\
&= \int_{\partial\Omega} (\boldsymbol{\sigma}\mathbf{n}) \cdot \mathbf{v} \; dA - \int_\Omega \boldsymbol{\sigma} : \nabla \mathbf{v} \; dV \\
&= \int_{\partial\Omega} \mathbf{t} \cdot \mathbf{v} \; dA - \int_\Omega \boldsymbol{\sigma} : \nabla \mathbf{v} \; dV = \int_{\partial\Omega} \mathbf{t} \cdot \mathbf{v} \; dA - \int_{\Omega_0} \boldsymbol{\tau} : \nabla \mathbf{v} \; dV_0 \\
&= \int_{\partial\Omega} \mathbf{t} \cdot \mathbf{v} \; dA - \int_{\Omega_0} \boldsymbol{\tau} : \nabla \mathbf{v}_E \; dV_0 - \int_{\Omega_0} \boldsymbol{\tau} : \nabla \mathbf{v}_P \; dV_0
\end{aligned}
$$

The time derivative of total energy $\dot{E}$ is then

$$
\begin{aligned}
\dot{E} = \dot{W} + \dot{E}_E &= \int_{\partial\Omega} \mathbf{t} \cdot \mathbf{v} \; dA - \int_{\Omega_0} \boldsymbol{\tau} : \nabla \mathbf{v}_E \; dV_0 - \int_{\Omega_0} \boldsymbol{\tau} : \nabla \mathbf{v}_P \; dV_0 + \int_{\Omega_0} \frac{\partial \psi(\mathbf{F}_E)}{\partial \mathbf{F}_E} : \dot{\mathbf{F}}_E \; dV_0 \\
&= \int_{\partial\Omega} \mathbf{t} \cdot \mathbf{v} \; dA - \int_{\Omega_0} \boldsymbol{\tau} : \nabla \mathbf{v}_E \; dV_0 - \int_{\Omega_0} \boldsymbol{\tau} : \nabla \mathbf{v}_P \; dV_0 + \int_{\Omega_0} \boldsymbol{\tau} : \nabla \mathbf{v}_E \; dV_0 \\
&= \int_{\partial\Omega} \mathbf{t} \cdot \mathbf{v} \; dA - \int_{\Omega_0} \boldsymbol{\tau} : \nabla \mathbf{v}_P \; dV_0
\end{aligned}
$$

Therefore $\int_{\Omega_0} \boldsymbol{\tau} : \nabla \mathbf{v}_P \; dV_0$ describes the *rate of dissipation.*

E Detailed measured stresses and yield surfaces

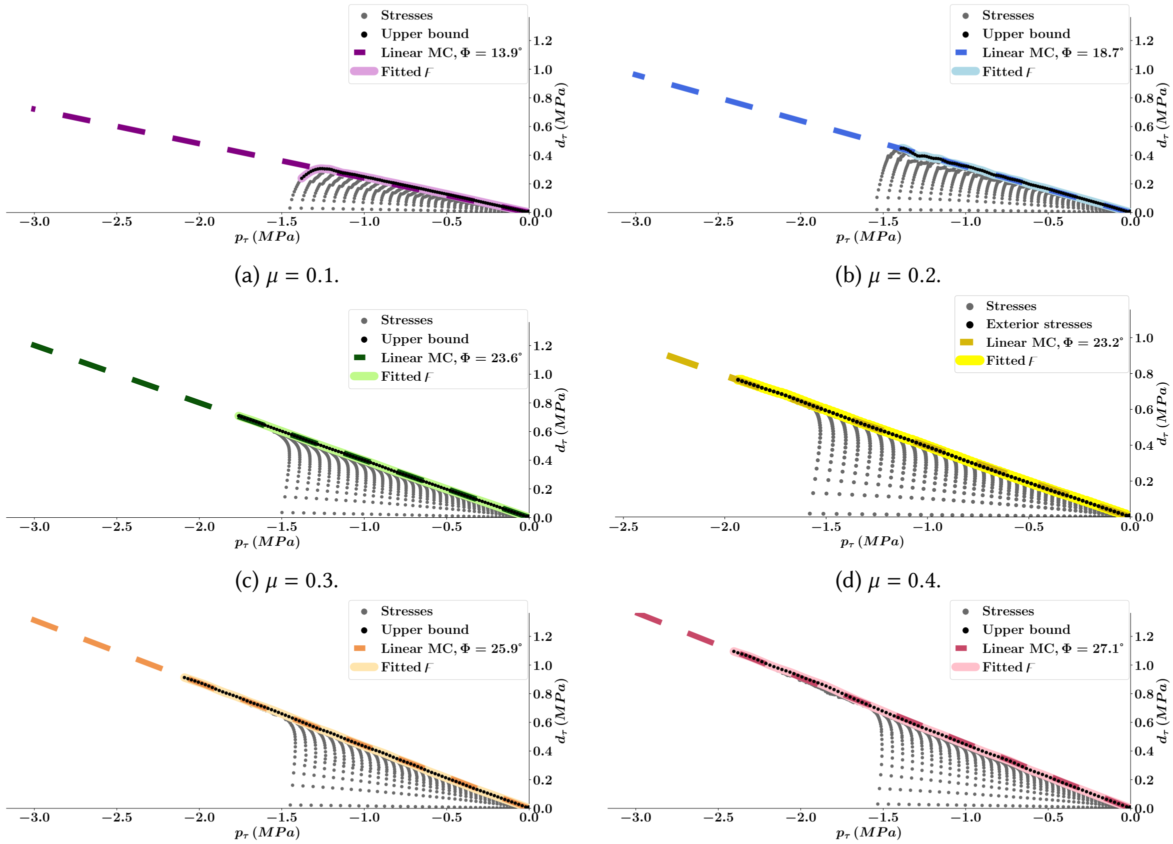

(a) $\mu = 0.1$.

(b) $\mu = 0.2$.

(c) $\mu = 0.3$.

(d) $\mu = 0.4$.

(e) $\mu = 0.5$.

(f) $\mu = 0.6$.

Fig. 1. Measured stresses and fitted linear Mohr–Coulomb and nonlinear Mohr–Coulomb $\mathcal{F}$ - Impact of the friction μ on monodisperse **Spheres**

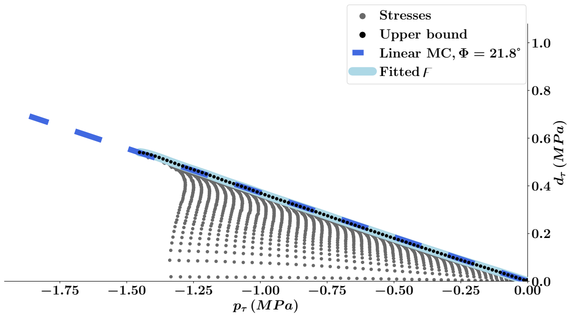

(a) $\mu = 0.2$.

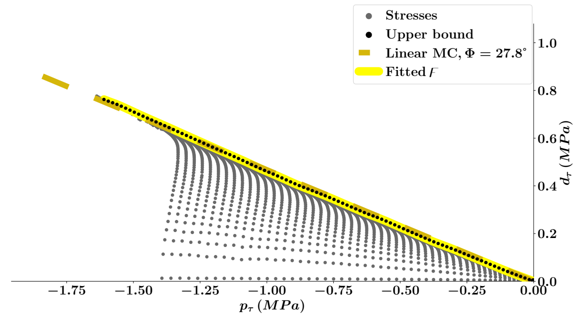

(b) $\mu = 0.4$.

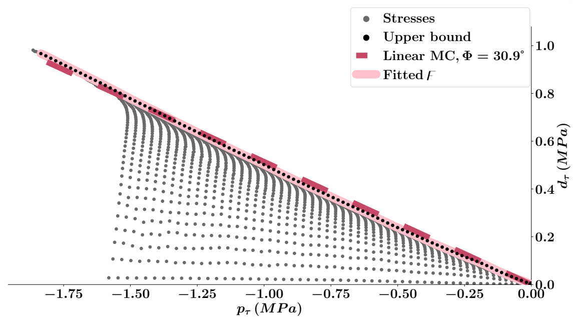

(c) $\mu = 0.6$.

Fig. 2. Measured stresses and fitted linear Mohr–Coulomb and nonlinear Mohr–Coulomb $\mathcal{F}$ - Impact of the friction μ on monodisperse **Spheres (linear spring)**.

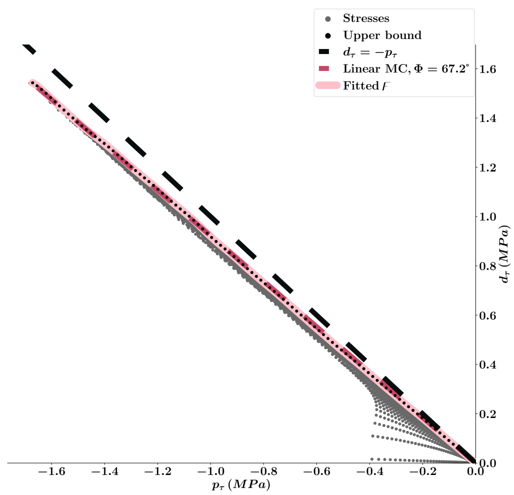

(a) **Dolosse**, $\mu = 0.6$.

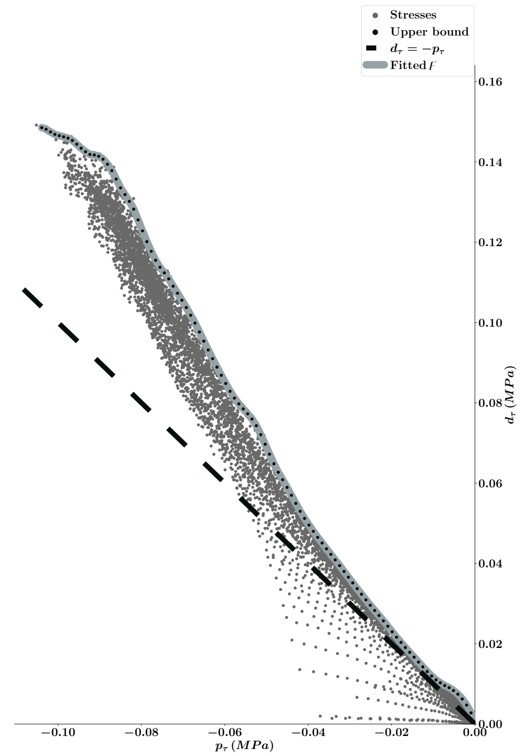

(b) **Dodecafangs**, $\mu = 0.8$.

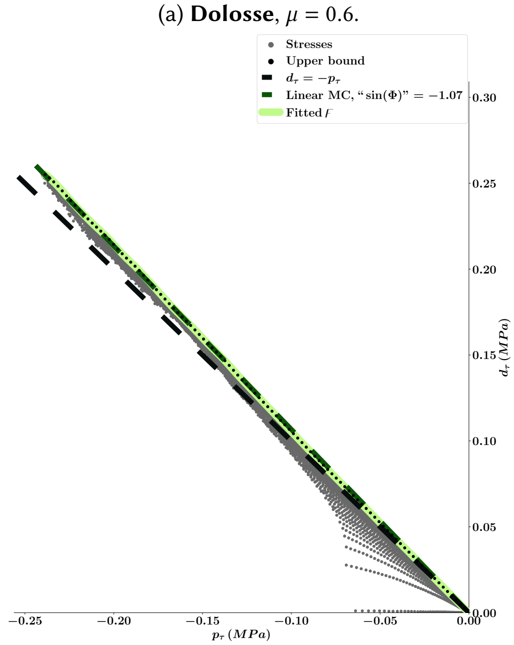

(c) **Hexapods**, $\mu = 0.3$.

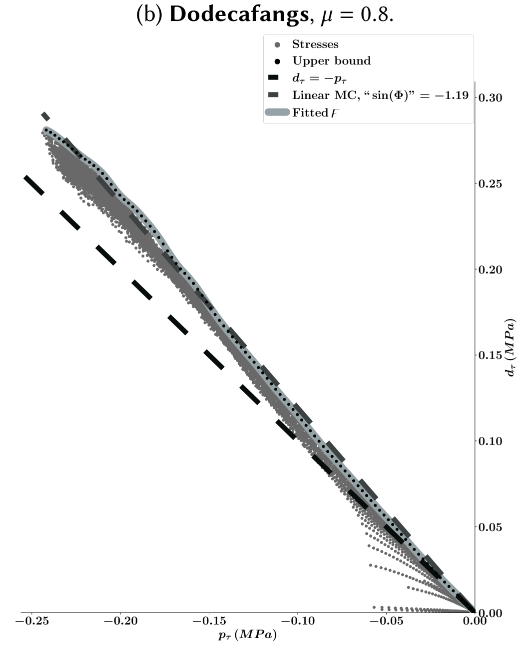

(d) **Hexapods**, $\mu = 0.8$.

Fig. 3. Measured stresses and fitted linear Mohr–Coulomb and nonlinear Mohr–Coulomb $\mathcal{F}$ - Nonconvex geometries

F Fitted elasticity parameters

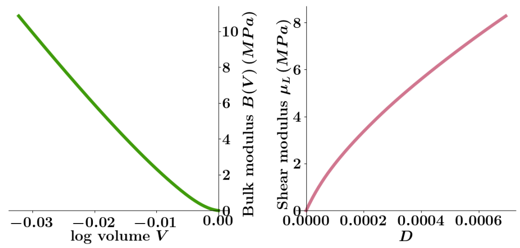

Fig. 4. Fitted bulk modulus $B(V)$ and shear modulus $\mu_{\mathrm{L}}(D)$ for **Spheres**, $\mu = 0.6$.

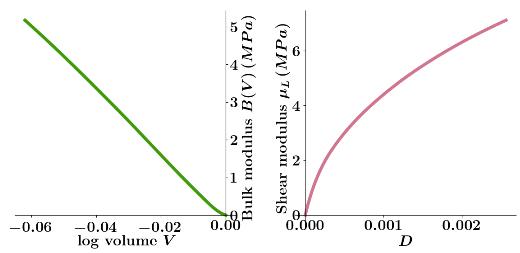

Fig. 5. Fitted bulk modulus $B(V)$ and shear modulus $\mu_{\mathrm{L}}(D)$ for **Dolosse**, $\mu = 0.6$.

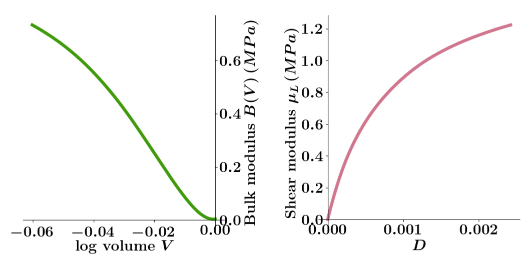

Fig. 6. Fitted bulk modulus $B(V)$ and shear modulus $\mu_{\mathrm{L}}(D)$ for **Hexapods**, $\mu = 0.8$.

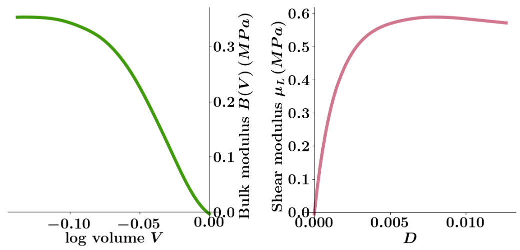

Fig. 7. Fitted bulk modulus $B(V)$ and shear modulus $\mu_{\mathrm{L}}(D)$ for **Dodecafangs**, $\mu = 0.8$.

G Detailed DEM results

G.1 Fitting slopes angles

For the inclined slopes and rotating drums examples, we numerically compute a slope angle as follows. For each timestep, we first project the spheres centers c_i in the xz-plane (camera plane in the renders). Then we optimize the line parameters (a, b) of the line $z = ax + b$ by minimizing

$$\min_{a,b} \sum_{(x_i,z_i)=c_i} D(ax_i - z_i + b) \qquad \text{with } D(x) = \begin{cases} \frac{1}{2}x^2 & \text{if } x \leq 0 \\ \exp(wx) - (1 + wx) & \text{otherwise} \end{cases} . \tag{38}$$

The function D ($w = 100$ in practice) acts as an asymmetric norm, encouraging the line to be close to the points but from above. For the slope angle, we report the first angle $\varphi = 180 \arctan(a)/\pi$ that differs with the container inclination angle by more than $\Phi_{\mathrm{A}}^{\epsilon} = 1°$. As described in the main paper, the drum consists in a cylinder of radius $\approx 2m$ and depth $\approx 1m$. With 10543 spheres of radius $4cm$, this results in $\approx 55 \times 15$ spheres at the free surface. The drum rotates at $90°/min$ and the friction between the spheres and the drum is set to $\mu = 0.6$.

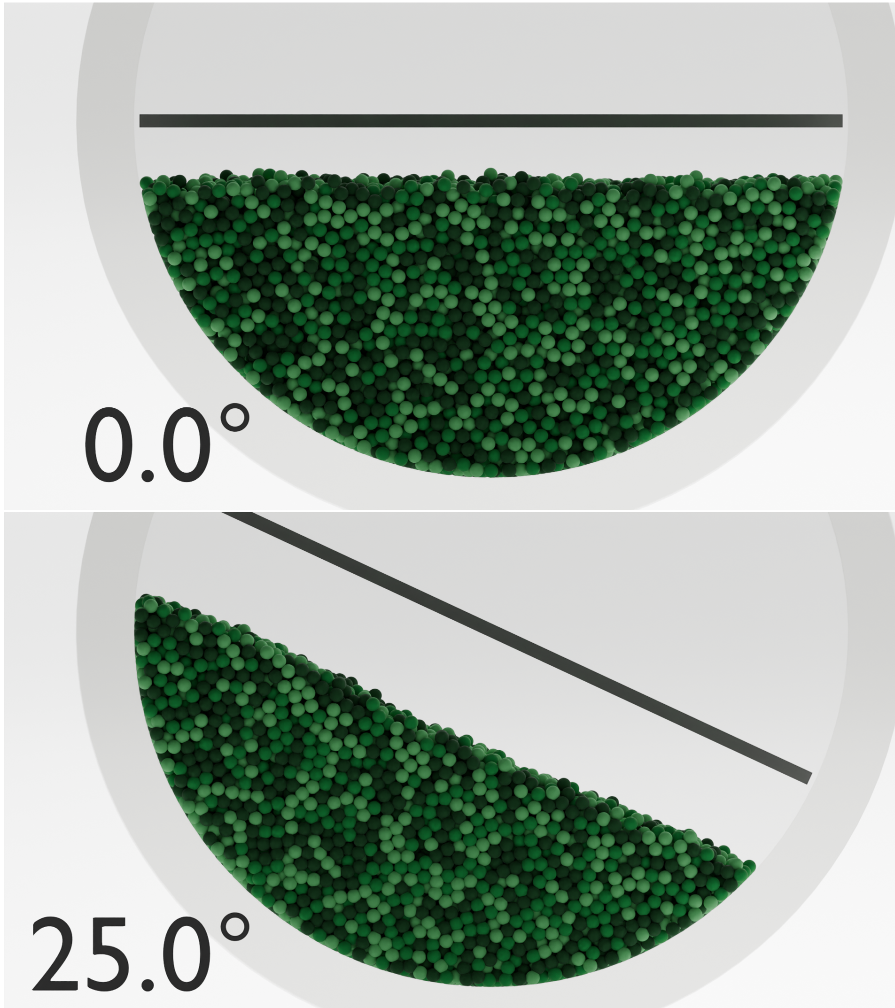

Fig. 8. Rotating drum setup.

G.2 Rotating drums angles for **Spheres**

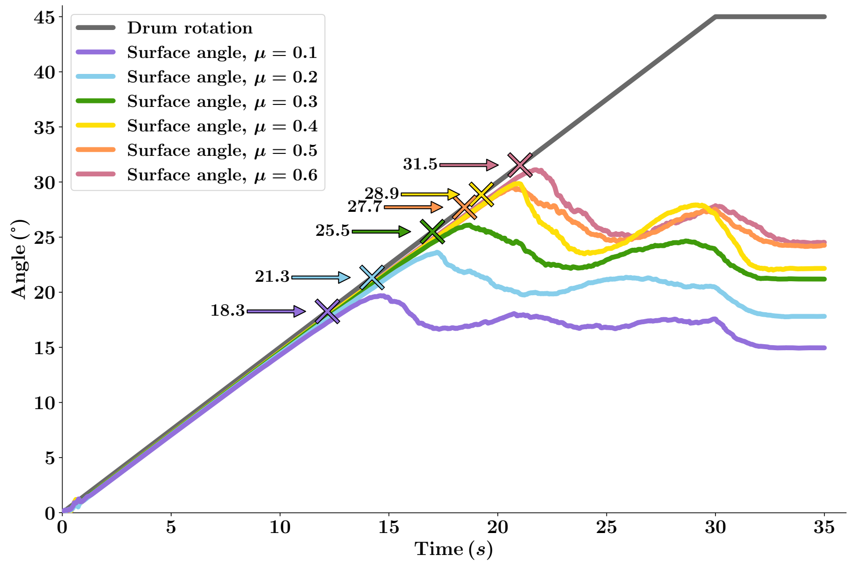

Fig. 9. **Spheres** example - Comparing the fitted surface angle from the DEM simulation to the container angle for varying grain friction μ. The crosses mark the computed avalanche angles Φ_A for $\Phi_A^{\varepsilon} = 1°$.

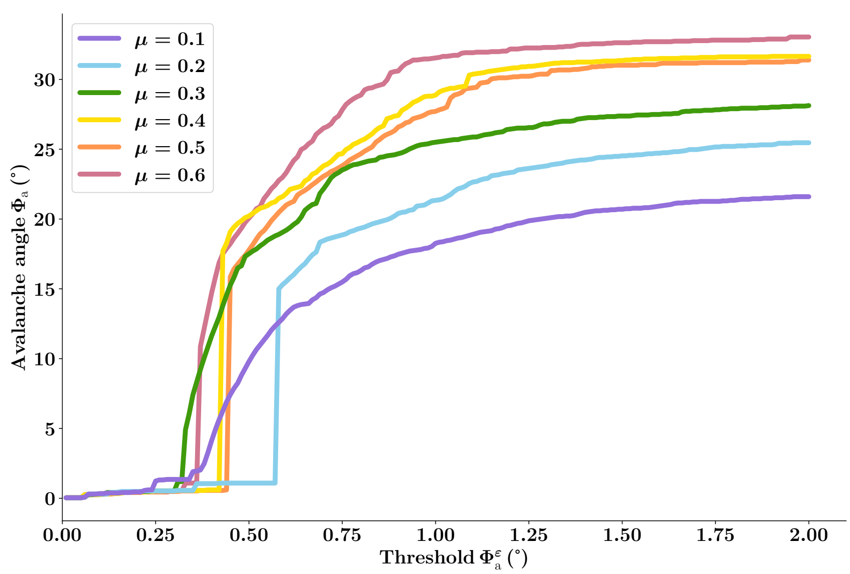

Fig. 10. **Spheres** example - Evolution of the detected avalanche angles Φ_A in function of the threshold Φ_A^{ε}.

G.3 Rotating drums angles for **Spheres (linear spring)**

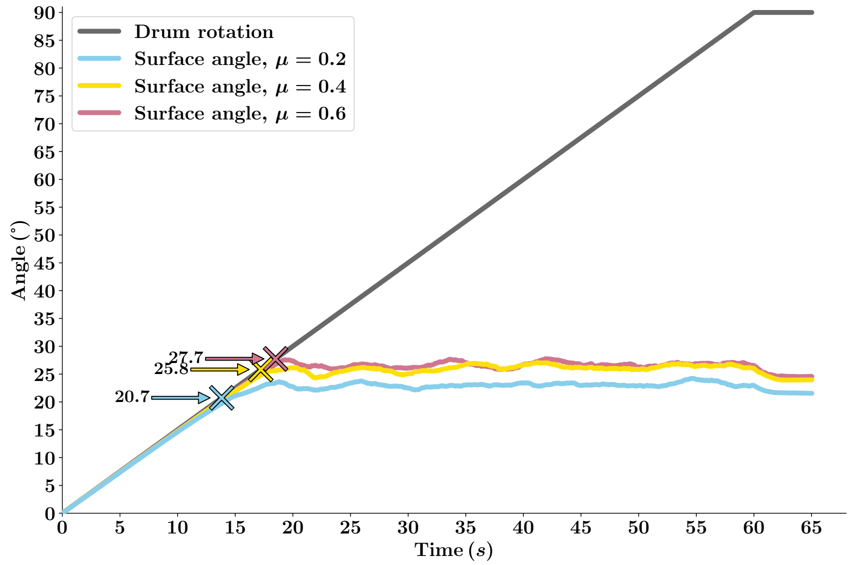

Fig. 11. **Spheres (linear spring)** example - Comparing the fitted surface angle from the DEM simulation to the container angle for varying grain friction μ. The crosses mark the computed avalanche angles Φ_A for $\Phi_A^{\varepsilon} = 1°$.

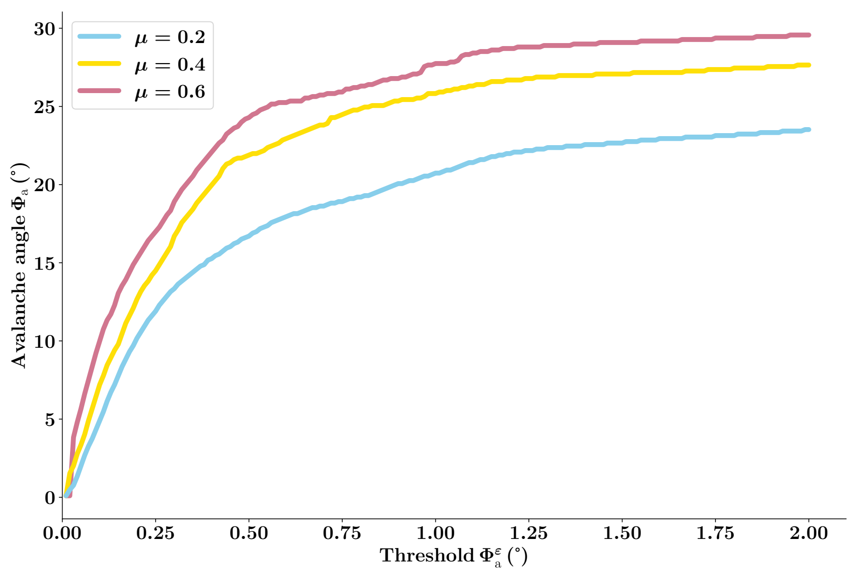

Fig. 12. **Spheres (linear spring)** example - Evolution of the detected avalanche angles Φ_A as a function of the threshold Φ_A^{ε}.

H Rendering

All results are rendered using Blender. For the rendering of our MPM simulations, each MPM particle is instantiated by a mesh of the corresponding grain shape. Each mesh follows a rigid body motion dictated by the particle properties, computed during the simulation and exported to a `NumPy` format used in Blender's Python scripting interface for rendering.

The position of the mesh is simply that of the MPM particle. The orientation $\mathbf{R}$ is extracted at each timestep from a polar decomposition of the particle's deformation gradient $\mathbf{F} = \mathbf{QR}$. That rotation matrix is composed with a random initial orientation $\mathbf{R_0}$ to give a more natural look to the whole sand pile.

Note that this technique works well for giving to the bulk the appearance of a sand made of the selected grain shape, but can produce visual artefacts visible under scrutiny of close-ups shots. Indeed, this technique yields visually intersecting grains or grains seemingly interacting although not in contact, as there is no real rigid body dynamic between the particles. The size of the mesh to use for instantiation is manually tuned to give the best appearance, but cannot totally remove these artefacts.

References

E.A. de Souza Neto, P.J. Blanco, P.J. Sánchez, and R.A. Feijóo. 2015. An RVE-based multiscale theory of solids with micro-scale inertia and body force effects. *Mechanics of Materials* 80 (2015), 136–144. doi:10.1016/j.mechmat.2014.10.007

R. Hill. 1963. Elastic properties of reinforced solids: Some theoretical principles. *Journal of the Mechanics and Physics of Solids* 11, 5 (1963), 357–372. doi:10.1016/0022-5096(63)90036-X

R. Hill. 1972. On Constitutive Macro-Variables for Heterogeneous Solids at Finite Strain. *Proceedings of the Royal Society of London. Series A, Mathematical and Physical Sciences* 326, 1565 (1972), 131–147. http://www.jstor.org/stable/78044

Jean Mandel. 1972. Plasticité classique et viscoplasticité. https://api.semanticscholar.org/CorpusID:118220241

accepted 25 September 2025